JOURNAL OF GUIDANCE, CONTROL, AND DYNAMICS
Vol. 21, No. 2, March–April 1998

Order-*N* Formulation and Dynamics of Multibody Tethered Systems

S. Kalantzis,* V. J. Modi,† and S. Pradhan‡
University of British Columbia, Vancouver, British Columbia V6T 1Z4, Canada
and
A. K. Misra§
McGill University, Montreal, Quebec H3A 2K6, Canada

The equations of motion for a multibody tethered satellite system in a three-dimensional Keplerian orbit are derived. The model considers a multisatellite system connected in series by flexible tethers. Both tethers and subsatellites are free to undergo three-dimensional attitude motion, together with deployment and retrieval as well as longitudinal and transverse vibration for the tether. The elastic deformations of the tethers are discretized using the assumed mode method. The tether attachment points to the subsatellites are kept arbitrary and time varying. The model is also capable of simulating the response of the entire system whose reference frames are spinning, initially in unison about an arbitrary axis, as in the case of OEDIPUS-A/C, which spins about the nominal tether length, or the proposed BICEPS mission where the system cartwheels about the orbit normal. The governing equations of motion are derived using an order-*N* Lagrangian procedure, which significantly reduces the computational cost associated with the inversion of the mass matrix, an important consideration for multisatellite systems. Finally, a symbolic integration and coding package is used to evaluate modal integrals, thus avoiding their costly on-line numerical evaluation.

Nomenclature

D_i	= magnitude of $\boldsymbol{D}_i$
$\boldsymbol{D}_i$	= inertial position vector of frame F_i
$\ddot{\boldsymbol{d}}_c$	= desired offset acceleration vector (ith link offset position)
$\boldsymbol{d}_i$	= position vector to the frame F_i from the frame F_{i-1}
dm_i	= infinitesimal mass element of the ith link
$d_{x_i}, d_{y_i}, d_{z_i}$	= Cartesian components of $\boldsymbol{d}_i$ along the local vertical, local horizontal, and orbit normal directions, respectively
F_i	= ith link body-fixed reference frame
F_0	= inertial reference frame
$\boldsymbol{g}_i$	= rigid and flexible position vectors of dm_i, $\boldsymbol{r}_i + \Phi_i \boldsymbol{\delta}_i$
I_{d_n}	= $n \times n$ identity matrix
$\hat{i}, \hat{j}, \hat{k}$	= unit vectors $\{1, 0, 0\}^T$, $\{0, 1, 0\}^T$, and $\{0, 0, 1\}^T$, respectively
l_i	= length of the ith link
$M(\boldsymbol{q}, t)$	= system's coupled mass matrix
M_t	= block diagonal decoupled mass matrix
m_i	= mass of the ith link
N	= total number of links
nq	= total number of generalized coordinates per link, $nf_i + 7$
nqq	= system's total number of generalized coordinates, Nnq
$n_{x_i}, n_{y_i}, n_{z_i}$	= number of flexible modes in the longitudinal, in-plane, and out-of-plane transverse directions, respectively, for the ith link
$\boldsymbol{q}$	= $\{\boldsymbol{q}_1^T, \ldots, \boldsymbol{q}_N^T\}^T$
$\boldsymbol{q}_i$	= set of generalized coordinates for the ith link that accounts for interactions with adjacent links
$\boldsymbol{q}_t$	= $\{\boldsymbol{q}_{t_1}^T, \ldots, \boldsymbol{q}_{t_N}^T\}^T$
$\boldsymbol{q}_{ti}$	= set of coordinates for the independent ith link (not connected to adjacent links)
$\boldsymbol{R}_{dm_i}$	= inertial position of the ith link mass element dm_i
R^p	= transformation matrix relating $\boldsymbol{q}_t$ and $\boldsymbol{q}$
R^v, R^n, R^d	= transformation matrices relating $\dot{\boldsymbol{q}}_t$ and $\dot{\boldsymbol{q}}$
$\boldsymbol{r}_i$	= rigid position of dm_i in the frame F_i
$\boldsymbol{T}_i$	= ith link rotation matrix
u_i, v_i, w_i	= flexible deformation of the ith link along the x_i, y_i, and z_i directions, respectively
x_i, y_i, z_i	= Cartesian components of $\boldsymbol{r}_i$
$\alpha_i, \beta_i, \gamma_i$	= pitch, roll, and yaw angles of the ith link
$\boldsymbol{\delta}_i(t)$	= time-varying modal coordinate for the ith flexible link
η_{d_i}	= structural damping coefficient for the ith link, E_{I_i}/E_i
$\boldsymbol{\eta}_i$	= set of attitude angles, $\{\alpha_i, \beta_i, \gamma_i\}^T$
$\boldsymbol{\Lambda}$	= Lagrangian multipliers
$\Phi_i(x_i, l_i)$	= matrix containing mode shape functions of the ith flexible link

Introduction

IN recent years, there has been a renewed interest in exploiting the gravity gradient environment in space. With that, research in tethered satellite systems is receiving considerable attention. Applications are numerous, from the study of Earth's ionosphere using probes lowered into the atmosphere from the Space Shuttle in a low Earth orbit, to the deployment of satellites or their retrieval for servicing. Even more promising applications of powering the proposed international space station by utilizing Earth's magnetic field are currently under study. Furthermore, tethers with multiple payloads have been proposed for monitoring Earth's environment in the global project, monitored by NASA, entitled Mission to Planet Earth. This has led to several studies aimed at multitethered systems.[1,2] In a recent study, Banerjee and Do[3] have considered an ocean-based system and applied a multibody algorithm to represent the tether flexibility. The present investigation adds to the current level of understanding in the general area of tethered satellite systems.

Presented as Paper 96-3571 at the AIAA/AAS Astrodynamics Specialist Conference, San Diego, CA, July 29–31, 1996; received Dec. 6, 1996; revision received Oct. 15, 1997; accepted for publication Oct. 18, 1997.

*Natural Sciences and Engineering Research Council Graduate Fellow, Department of Mechanical Engineering.
†Professor Emeritus, Department of Mechanical Engineering. Fellow AIAA.
‡Postdoctoral Fellow, Department of Mechanical Engineering.
§Professor, Department of Mechanical Engineering. Associate Fellow AIAA.

In modeling of a multibody system, the degrees of freedom increase dramatically as bodies are added. Representation of attitude motion together with suitable discretization for flexibility results in a large number of generalized coordinates, thus requiring the solution of an extensive set of governing equations of motion. This leads to lengthy simulation times and almost no possibility of real-time control implementation. It has become increasingly clear that the question of computational efficiency in the dynamics formulation must be addressed.

Fortunately, in the past two decades, there has been a concerted effort at developing efficient algorithms to study the forward and inverse dynamics of multibody systems. Several efficient dynamic formulations have been developed where the computational effort for generating the acceleration vector of each generalized coordinate varies linearly with the number of bodies N. This is referred to as an order-N, $\mathcal{O}(N)$, formulation.

The first $\mathcal{O}(N)$ dynamic formulation was based on a Newton–Euler approach[4] and was aimed at the multilink equations of motion. It involved a sequential or recursive forward pass along the links to calculate the acceleration vector, followed by a backward pass that accounted for the constraint forces between the links. Hollerbach[5] proposed a recursive formulation; however, it was based on Lagrange's equations of motion. His algorithm was $\mathcal{O}(N)$ for the inverse dynamics but not for the forward dynamics. Rosenthal[6] also proposed an $\mathcal{O}(N)$ algorithm, based on Kane's equations of motion for a chain link topology, but he encountered some difficulty in implementing flexibility in the model. Banerjee[7] proposes a significant advancement of Rosenthal's recursive approach, overcoming the original flexibility shortcomings of Rosenthal's method in addition to further decomposition of the mass matrix using Kane's approach, leading to an improved $\mathcal{O}(N)$ algorithm.

Keat[8] has reported an $\mathcal{O}(N)$ recursive algorithm, for the Newton–Euler equations, based on a velocity transformation. The introduction of a spatial operator factorization,[9,10] which utilizes an analogy between multibody robot dynamics and linear filtering and smoothing theory, to efficiently invert the system's mass matrix is another approach to a recursive algorithm. On the other hand, a nonrecursive formulation utilizing the range space method,[11] which employs element-by-element methods in use in finite element procedures, has also been considered, thus illustrating a variety in approaches developed over the years.

The algorithm presented in this paper uses a variable transformation approach to factorize the system's mass matrix[12] and is extended for the case of variable length links. The resulting set of Lagrangian equations of motion are nonrecursive in nature, permitting parallel computation as the governing equations for the individual body are independent. Two different velocity transformations are used for computing the mass matrix and its inverse.

The model considers a multisatellite system, connected by tethers forming a chain-type topology, in an arbitrary orbit around Earth, as shown in Fig. 1. The system is free to undergo three-dimensional librational motion, including spin about an arbitrary axis (cartwheeling). Furthermore, the platform, tether, and subsatellite are capable of three-dimensional rigid-body motion in addition to longitudinal and transverse elastic vibrations for the tether. The flexible motion is discretized using the assumed mode method[13] where foreshortening effects due to geometric stiffness are included. Several discretization schemes have been presented by other researchers, including a lumped-mass or bead model,[14] a hybrid bead/continuum model,[1] a finite element approach,[15] and others. As can be expected, each of these methods has its merit. Here a continuum model is chosen for its simplicity and proven desirable performance.

To improve the performance further, a symbolic manipulation package (Maple V) was used to evaluate the modal integrals involving the admissible functions describing the flexible motion. This allowed direct coding of the integrated functions, instead of their numerical evaluation during the simulation. The result was a significant reduction in computational time, especially during deployment and retrieval.

Description of System

The derivation of the equations of motion begins with the definition of the kinetic energy of an arbitrary link of the multibody system. Let the ith link of the system be free to translate and to rotate in three-dimensional space. From Fig. 2, the vector $\boldsymbol{R}_{dm_i}$ to the mass element dm_i on the ith link, relative to the inertial frame F_0, can be written as

$$\boldsymbol{R}_{dm_i} = \boldsymbol{D}_i + \boldsymbol{T}_i\left\{\boldsymbol{r}_i + \boldsymbol{f}_i^f(\boldsymbol{r}_i)\right\} \tag{1}$$

where $\boldsymbol{f}_i^f(\boldsymbol{r}_i)$ is the flexible deformation at $\boldsymbol{r}_i$. Note, in the present model, tethers (i even) are considered flexible, whereas the subsatellite payloads (i odd) are taken to be rigid, i.e., $\boldsymbol{f}_i^f(\boldsymbol{r}_i) \equiv 0$. As mentioned earlier, the tether flexibility is discretized using the assumed mode method as

$$f_i^f(\boldsymbol{r}_i) = \begin{pmatrix} u_i \\ v_i \\ w_i \end{pmatrix} = \Phi_i(x_i)\boldsymbol{\delta}_i(t) \tag{2}$$

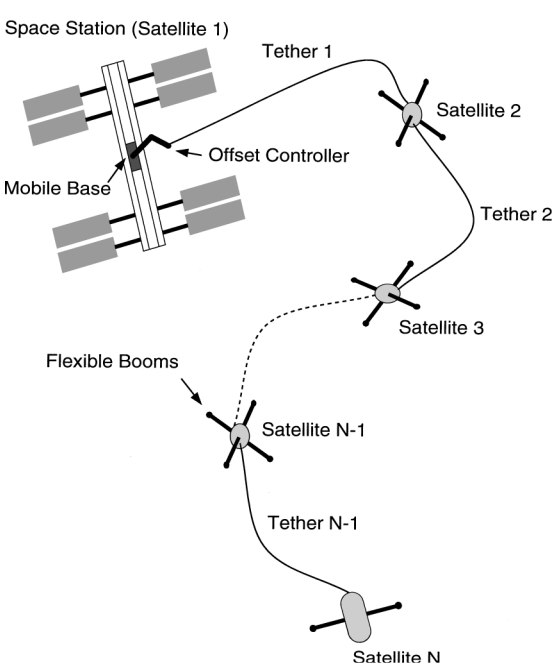

Fig. 1 Schematic diagram of the space station-based N-body tethered satellite system.

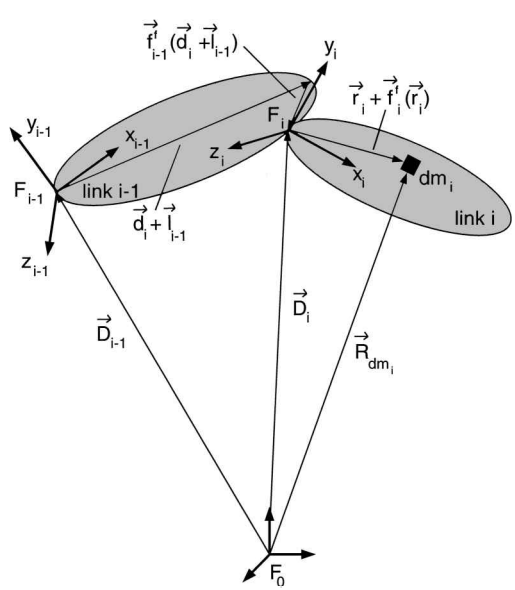

Fig. 2 Vector components of the ith and $(i-1)$th chain link.

where $\Phi_i(x_i)$ is the matrix of the tether mode shape functions. For the jth longitudinal mode, the admissible function[16] is taken as

$$\Phi_u^j(x_i) = (x_i/l_i)^{2j-1} \tag{3}$$

In the case of in-plane and out-of-plane transverse deflections, the admissible functions are

$$\Phi_v^j(x_i) = \Phi_w^j(x_i) = \sqrt{2}\sin(j\pi x_i/l_i) \tag{4}$$

where $\sqrt{2}$ is added as a normalizing factor. Thus

$$\Phi_i(x_i, l_i) = \begin{bmatrix} \Phi_{x_i}^1 \cdots \Phi_{x_i}^{n_{x_i}} & 0 & 0 \\ 0 & \Phi_{y_i}^1 \cdots \Phi_{y_i}^{n_{y_i}} & 0 \\ 0 & 0 & \Phi_{z_i}^1 \cdots \Phi_{z_i}^{n_{z_i}} \end{bmatrix} \in \Re^{3\times nf_i} \tag{5}$$

where $nf_i = n_{x_i} + n_{y_i} + n_{z_i}$ and n_{x_i}, n_{y_i}, and n_{z_i} are the number of modes used in the longitudinal, in-plane, and out-of-plane transverse directions, respectively. The time-varying modal coordinate vector $\boldsymbol{\delta}_i$ in Eq. (2) is composed of the longitudinal and transverse generalized coordinates associated with the corresponding mode of vibration such that

$$\boldsymbol{\delta}_i = \begin{pmatrix} \boldsymbol{\delta}_{x_i} \\ \boldsymbol{\delta}_{y_i} \\ \boldsymbol{\delta}_{z_i} \end{pmatrix} \in \Re^{3\times nf_i} \tag{6}$$

The matrix $\boldsymbol{T}_i$ in Eq. (1) represents a rotation transformation from the body-fixed frame F_i to the inertial frame F_0, i.e., $F_0 = \boldsymbol{T}_i F_i$. It is defined by the 3-2-1 sequence of elementary rotations[17] as

$$\boldsymbol{T}_i = \begin{bmatrix} C_{\beta_i}C_{\alpha_i} & -C_{\gamma_i}S_{\alpha_i} + S_{\gamma_i}S_{\beta_i}S_{\alpha_i} & S_{\gamma_i}S_{\alpha_i} + C_{\gamma_i}S_{\beta_i}C_{\alpha_i} \\ C_{\beta_i}S_{\alpha_i} & C_{\gamma_i}C_{\alpha_i} + S_{\gamma_i}S_{\beta_i}S_{\alpha_i} & -S_{\gamma_i}C_{\alpha_i} + C_{\gamma_i}S_{\beta_i}S_{\alpha_i} \\ -S_{\beta_i} & S_{\gamma_i}C_{\beta_i} & C_{\gamma_i}C_{\beta_i} \end{bmatrix} \tag{7}$$

where α_i is the in-plane (pitch) angle, β_i is the out-of-plane (roll) angle, and γ_i is the spin (yaw) angle. The terms C_x and S_x are abbreviations for $\cos(x)$ and $\sin(x)$, respectively.

Letting $\boldsymbol{g}_i = \boldsymbol{r}_i + \Phi_i\boldsymbol{\delta}_i$ and differentiating Eq. (1) with respect to time give

$$\dot{\boldsymbol{R}}_{dm_i} = \dot{\boldsymbol{D}}_i + P_i(\boldsymbol{g}_i)\dot{\boldsymbol{\eta}}_i + \boldsymbol{T}_i\Phi_i\dot{\boldsymbol{\delta}}_i + \boldsymbol{T}_i\boldsymbol{s}_i\dot{l}_i \tag{8}$$

where $\boldsymbol{s}_i = \hat{i} + \Phi_{D_i}\boldsymbol{\delta}_i$, $\Phi_{D_i} = [(\partial/\partial x_i) + (\partial/\partial l_i)]\Phi_i$, and l_i is the length of the ith link. Finally, letting $\boldsymbol{\eta}_i = [\alpha_i, \beta_i, \gamma_i]^T$, then the column matrix $P_i(\boldsymbol{g}_i)$ can be defined as

$$P_i(\boldsymbol{g}_i)\dot{\boldsymbol{\eta}}_i = \dot{\boldsymbol{T}}_i\boldsymbol{g}_i = \left[T_{\alpha_i}\boldsymbol{g}_i, T_{\beta_i}\boldsymbol{g}_i, T_{\gamma_i}\boldsymbol{g}_i\right]\dot{\boldsymbol{\eta}}_i \tag{9}$$

where $T_{\alpha_i} = (\partial/\partial\alpha_i)\boldsymbol{T}_i$, $T_{\beta_i} = (\partial/\partial\beta_i)\boldsymbol{T}_i$, and $T_{\gamma_i} = (\partial/\partial\gamma_i)\boldsymbol{T}_i$.

Kinetic Energy

The kinetic energy of the ith link can now be obtained from Eq. (8) as

$$K_{e_i} = \frac{1}{2}\int_{m_i} \dot{\boldsymbol{R}}_{dm_i}^T\dot{\boldsymbol{R}}_{dm_i}\,dm_i \tag{10}$$

Setting Eq. (8) in a matrix form gives the relation

$$\dot{\boldsymbol{R}}_{dm_i} = \begin{bmatrix} I_{d_3} & P_i(\boldsymbol{g}_i) & \boldsymbol{T}_i\Phi_i & \boldsymbol{T}_i\boldsymbol{s}_i \end{bmatrix}\dot{\boldsymbol{q}}_{t_i} \tag{11}$$

where I_{d_3} is the 3×3 identity matrix and

$$\dot{\boldsymbol{q}}_{t_i} = \begin{pmatrix} \dot{\boldsymbol{D}}_{s_i} \\ \dot{\boldsymbol{\eta}}_i \\ \dot{\boldsymbol{\delta}}_i \\ \dot{l}_i \end{pmatrix} \in \Re^{nq\times 1} \tag{12}$$

Inserting Eq. (11) into Eq. (10) and integrating, the kinetic energy for the ith link can be written as

$$K_{e_i} = \tfrac{1}{2}\dot{\boldsymbol{q}}_{t_i}^T M_{t_i}\dot{\boldsymbol{q}}_{t_i} \tag{13}$$

where

$$M_{t_i} = \begin{bmatrix} m_i I_{d_3} & P_i\left(\int \boldsymbol{g}_i dm_i\right) & \boldsymbol{T}_i\int \Phi_i dm_i & \boldsymbol{T}_i\int \boldsymbol{s}_i dm_i \\ \text{sym} & \int P_i^T(\boldsymbol{g}_i)P_i(\boldsymbol{g}_i)dm_i & \int P_i^T(\boldsymbol{g}_i)\boldsymbol{T}_i\Phi_i dm_i & \int P_i^T(\boldsymbol{g}_i)\boldsymbol{T}_i\boldsymbol{s}_i dm_i \\ \text{sym} & \text{sym} & \int \Phi_i^T\Phi_i dm_i & \int \Phi_i^T\boldsymbol{s}_i dm_i \\ \text{sym} & \text{sym} & \text{sym} & \int \boldsymbol{s}_i^T\boldsymbol{s}_i dm_i \end{bmatrix} \in \Re^{nq\times nq} \tag{14}$$

The kinetic energy for the entire system, i.e., N bodies, can now be stated as

$$K_e = \frac{1}{2}\sum_{i=1}^{N}\dot{\boldsymbol{q}}_{t_i}^T M_{t_i}\dot{\boldsymbol{q}}_{t_i} = \frac{1}{2}\dot{\boldsymbol{q}}_t^T M_t\dot{\boldsymbol{q}}_t \tag{15}$$

where $\boldsymbol{q}_t = \{\boldsymbol{q}_{t_1}^T, \boldsymbol{q}_{t_2}^T, \ldots, \boldsymbol{q}_{t_N}^T\}^T$ and M_t is a block diagonal matrix with M_{t_i} on its diagonal.

Note that, for rigid links, this symmetric mass matrix is considerably simpler and can be described in terms of the center of mass and inertia tensor of each link. Also, the kinetic energy expression in Eq. (15) has a quadratic form from which it can be easily manipulated to obtain the final form of the equations of motion. Finally, most integrals in Eq. (14) can be evaluated symbolically and hence coded directly in Fortran.

Gravitational Potential Energy

The gravitational potential energy of the ith link, due to the central force law, is given as

$$V_{g_i} = -\mu\int_{m_i}\frac{dm_i}{\left|\boldsymbol{R}_{dm_i}\right|} \tag{16}$$

where $\mu = 3.986\times 10^5$ km^3/s^2 is Earth's gravitational constant. Using the binomial expansion and retaining terms up to third order give

$$V_{g_i} = \frac{-\mu m_i}{D_i} + \frac{\mu}{2D_i^3}\left[\int \boldsymbol{g}_i^T\boldsymbol{g}_i dm_i + 2\boldsymbol{D}_i^T\boldsymbol{T}_i\int \boldsymbol{g}_i dm_i - \frac{3}{D_i^2}\boldsymbol{D}_i^T\boldsymbol{T}_i\int \boldsymbol{g}_i\boldsymbol{g}_i^T dm_i\boldsymbol{T}_i^T\boldsymbol{D}_i\right] \tag{17}$$

which is in terms of symbolically evaluated integrals.

Strain Energy

The tether strain-displacement relationship can be written as

$$\varepsilon_i = \frac{\partial u_i}{\partial x_i} + \frac{1}{2}\left[\left(\frac{\partial v_i}{\partial x_i}\right)^2 + \left(\frac{\partial w_i}{\partial x_i}\right)^2\right] \tag{18}$$

where u_i, v_i, and w_i are obtained from Eq. (2) and $\varepsilon_i > 0$ because compression is not supported by any tether. The second bracketed term in Eq. (18) represents the geometric nonlinearity and is responsible for the foreshortening effects in the tether. It cannot be neglected because of the relatively large amplitude motions encountered in the tether dynamics. The strain energy is given by

$$V_{e_i} = \frac{1}{2} E_i A_i \int_0^{l_i} \varepsilon_i^2 \, \mathrm{d}x_i \tag{19}$$

where $E_i A_i$ is the tether flexural stiffness. The total potential energy of the system is

$$P_e = \sum_{n=1}^{N} \left(V_{g_i} + V_{e_i}\right)$$

Tether Dissipation

The dissipation of energy due to longitudinal elastic vibration of the tether can be described by the Rayleigh dissipation function[16]

$$W_{d_i} = \frac{1}{2} \frac{E_i A_i \eta_{d_i}}{\omega_i} \int_0^{l_i} (\dot{\varepsilon}_i)^2 \tag{20}$$

where η_{d_i} and ω_i are the structural damping coefficient and the fundamental oscillation frequency of the ith tether, respectively. The strain rate $\dot{\varepsilon}_i$ is the time derivative of Eq. (18). The generalized external force due to damping can now be defined as $\boldsymbol{Q}_d = \{\boldsymbol{Q}_{d_1}^T, \ldots, \boldsymbol{Q}_{d_N}^T\}^T$, where

$$\begin{aligned} \boldsymbol{Q}_{d_i} &= -\frac{\partial W_{d_i}}{\partial \dot{\boldsymbol{q}}_i}, \qquad i = 2, 4, \ldots, N-1 \\ &= 0, \qquad\qquad i = 1, 3, \ldots, N \end{aligned} \tag{21}$$

Lagrangian Equations of Motion

With the energy expressions in hand, the equations of motion can be obtained quite readily using the Lagrangian principle

$$\frac{\mathrm{d}}{\mathrm{d}t}\left(\frac{\partial K_e}{\partial \dot{\boldsymbol{q}}}\right) - \frac{\partial (K_e - P_e)}{\partial \boldsymbol{q}} = \boldsymbol{Q} + \boldsymbol{Q}_d \tag{22}$$

Substituting Eqs. (15), (17), (19), and (21) into Eq. (22) leads to the familiar matrix form of the coupled equations of motion for the system:

$$M(\boldsymbol{q})\ddot{\boldsymbol{q}} + \boldsymbol{F}(\boldsymbol{q}, \dot{\boldsymbol{q}}) = \boldsymbol{Q}(\boldsymbol{q}, \dot{\boldsymbol{q}}) \tag{23}$$

where M is the nonlinear symmetric mass matrix; $\boldsymbol{F}(\boldsymbol{q}, \dot{\boldsymbol{q}})$ is the forcing vector function given by

$$\boldsymbol{F}(\boldsymbol{q}, \dot{\boldsymbol{q}}, t) = \dot{M}\dot{\boldsymbol{q}} - \frac{1}{2}\dot{\boldsymbol{q}}^T \frac{\partial M}{\partial \boldsymbol{q}}\dot{\boldsymbol{q}} + \frac{\partial \boldsymbol{q}_t}{\partial \boldsymbol{q}} \frac{\partial P_e}{\partial \boldsymbol{q}_t} - \boldsymbol{Q}_d \tag{24}$$

The term $\boldsymbol{Q}(\boldsymbol{q}, \dot{\boldsymbol{q}})$ is the vector of generalized external forces, including control inputs, acting on the system.

Numerical solution of Eq. (23) in terms of $\ddot{\boldsymbol{q}}$ requires the inversion of the mass matrix. However, M is a full matrix of size $nqq \times nqq$, where $nqq = Nnq$ and is the total number of generalized coordinates in the system; nq is the number of degrees of freedom for each body. Therefore, direct inversion of M would lead to a large number of computation steps of the order nqq^3 or higher. The objective here is to develop an order-N, $\mathcal{O}(N)$, algorithm for obtaining M^{-1} that minimizes the computational effort. This is accomplished through the following transformations.

Coordinate Transformations

When deriving the energy expressions of the system, the focus is on the decoupled system, i.e., each link is considered independent of the others. Thus each link's energy expression is also uncoupled from the others. However, the interconnecting constraint forces must be incorporated into the final equations.

Let

$$\boldsymbol{q}_i = \begin{pmatrix} \boldsymbol{d}_i \\ \boldsymbol{\eta}_i \\ \boldsymbol{\delta}_i \\ l_i \end{pmatrix} \in \Re^{nq \times 1} \tag{25}$$

be the vector of coupled coordinates of the ith link such that $\boldsymbol{q} = \{\boldsymbol{q}_1^T, \boldsymbol{q}_2^T, \ldots, \boldsymbol{q}_N^T\}^T$ is the system's generalized coordinates. Let $\boldsymbol{q}_{t_i}$ be the set of auxiliary decoupled coordinates such that $\boldsymbol{q}_t = \{\boldsymbol{q}_{t_1}^T, \boldsymbol{q}_{t_2}^T, \ldots, \boldsymbol{q}_{t_N}^T\}^T$. The only difference between $\boldsymbol{q}_{t_i}$ and $\boldsymbol{q}_i$ is $\boldsymbol{D}_i$ and $\boldsymbol{d}_i$. The term $\boldsymbol{D}_i$ is the inertial position of F_i from F_0, whereas $\boldsymbol{d}_i = \{d_{x_i}, d_{y_i}, d_{z_i}\}^T$ is defined as the offset position of F_i relative to F_{i-1}.

Position Transformation

From Fig. 2,

$$\boldsymbol{D}_i = \boldsymbol{D}_{i-1} + \boldsymbol{T}_{i-1}\{l_{i-1}\hat{i} + \boldsymbol{d}_i\} + \boldsymbol{T}_{i-1}\Phi_{i-1}\left(l_{i-1} + d_{x_i}\right)\boldsymbol{\delta}_{i-1} \tag{26}$$

where d_{x_i} is the x_i component of $\boldsymbol{d}_i$. Defining $KA_{i-1} = \Phi_{i-1}(l_{i-1} + d_{x_i})$, Eq. (26) can be rewritten in summation form as

$$\boldsymbol{D}_i = \sum_{j=1}^{i} (\boldsymbol{T}_{j-1}\boldsymbol{d}_j + \boldsymbol{T}_{j-1} KA_{j-1}\boldsymbol{\delta}_{j-1} + \boldsymbol{T}_{j-1}\hat{i} l_{j-1}) \tag{27}$$

Introducing the index substitution $k = j - 1$, Eq. (27) can be rewritten as

$$\boldsymbol{D}_i = \sum_{k=1}^{i-1} (\boldsymbol{T}_{k-1}\boldsymbol{d}_k + \boldsymbol{T}_k KA_k\boldsymbol{\delta}_k + \boldsymbol{T}_k \hat{i} l_k) + \boldsymbol{T}_{i-1}\boldsymbol{d}_i \tag{28}$$

because $\boldsymbol{d}_1 = \boldsymbol{D}_1$, $\boldsymbol{T}_0 = I_{d_3}$, and l_0, $\boldsymbol{D}_0$, and $\boldsymbol{\delta}_0$ are null vectors. Recasting Eq. (28) in matrix form leads to

$$\boldsymbol{q}_{t_i} = \sum_{k=1}^{i-1} \left(R_k^p \boldsymbol{q}_k\right) + R_i \boldsymbol{q}_i \tag{29}$$

where

$$R_k^p = \begin{bmatrix} \boldsymbol{T}_{k-1} & 0 & \boldsymbol{T}_k KA_k & \boldsymbol{T}_k \hat{i} \\ 0 & 0 & 0 & 0 \\ 0 & 0 & 0 & 0 \\ 0 & 0 & 0 & 0 \end{bmatrix} \in \Re^{nq \times nq} \tag{30}$$

and

$$R_i = \begin{bmatrix} \boldsymbol{T}_{i-1} & 0 & 0 & 0 \\ 0 & I_{d_3} & 0 & 0 \\ 0 & 0 & I_{d_{nf_i}} & 0 \\ 0 & 0 & 0 & 1 \end{bmatrix} \in \Re^{nq \times nq} \tag{31}$$

For the entire system,

$$\boldsymbol{q}_t = R^p \boldsymbol{q} \tag{32}$$

where

$$R^p = \begin{bmatrix} R_1 & 0 & 0 & \cdots & 0 \\ R_1^p & R_2 & 0 & \cdots & 0 \\ R_1^p & R_2^p & R_3 & \cdots & 0 \\ \vdots & \vdots & \ddots & \ddots & \vdots \\ R_1^p & R_2^p & \cdots & R_{N-1}^p & R_N \end{bmatrix} \in \Re^{nqq \times nqq} \tag{33}$$

and R^p is the lower triangular block matrix that relates $\boldsymbol{q}_t$ and $\boldsymbol{q}$.

Velocity Transformations

The two sets of velocity coordinates $\dot{\boldsymbol{q}}_{t_i}$ and $\dot{\boldsymbol{q}}_i$ are related by the following two transformations.

First Transformation

Differentiating Eq. (26) with respect to time gives the inertial velocity of the ith link as

$$\dot{\boldsymbol{D}}_i = \dot{\boldsymbol{D}}_{i-1} + \boldsymbol{T}_{i-1}\left\{I_{d_3} + KAD_{i-1}\boldsymbol{\delta}_{i-1}\hat{i}^T\right\}\dot{\boldsymbol{d}}_i + P_{i-1}(\boldsymbol{h}_{i-1})\dot{\boldsymbol{\eta}}_{i-1} + \boldsymbol{T}_{i-1}KA_{i-1}\dot{\boldsymbol{\delta}}_{i-1} + \boldsymbol{T}_{i-1}\{\hat{i} + KAL_{i-1}\boldsymbol{\delta}_{i-1}\}\dot{l}_{i-1} \tag{34}$$

where $KAD_i = \partial/\partial d_{x_{i+1}}\{KA_i\}$, $KAL_i = \partial/\partial l_i\{KA_i\}$, and $\boldsymbol{h}_i = \boldsymbol{d}_{i+1} + l_i\hat{i} + KA_i\boldsymbol{\delta}_i$.

Following a procedure similar to the one used during the position transformation derivation, it can be shown that

$$\dot{\boldsymbol{q}}_t = R^v\dot{\boldsymbol{q}} \tag{35}$$

where R^v is given by the following lower triangular block matrix:

$$R^v = \begin{bmatrix} R_1^d & 0 & 0 & \cdots & 0 \\ R_1^v & R_2^d & 0 & \cdots & 0 \\ R_1^v & R_2^v & R_3^d & \cdots & 0 \\ \vdots & \vdots & \ddots & \ddots & \vdots \\ R_1^v & R_2^v & \cdots & R_{N-1}^v & R_N^d \end{bmatrix} \in \Re^{nqq\times nqq} \tag{36}$$

Here

$$R_i^v = \begin{bmatrix} \boldsymbol{T}_{i-1}KD_{i-1} & P_i(\boldsymbol{h}_i) & \boldsymbol{T}_iKA_i & \boldsymbol{T}_iKL_i \\ 0 & 0 & 0 & 0 \\ 0 & 0 & 0 & 0 \\ 0 & 0 & 0 & 0 \end{bmatrix} \in \Re^{nq\times nq} \tag{37}$$

and

$$R_i^d = \begin{bmatrix} \boldsymbol{T}_{i-1}KD_{i-1} & 0 & 0 & 0 \\ 0 & I_{d_3} & 0 & 0 \\ 0 & 0 & I_{d_{nf_i}} & 0 \\ 0 & 0 & 0 & 1 \end{bmatrix} \in \Re^{nq\times nq} \tag{38}$$

where $KD_{i-1} = I_{d_3} + KAD_{i-1}\boldsymbol{\delta}_{i-1}\hat{i}^T$ and $KL_i = \hat{i} + KAL_i\boldsymbol{\delta}_i$.

Second Transformation

The second transformation is simply Eq. (34) set into matrix form. This leads to the expression for $\dot{\boldsymbol{q}}_{t_i}$ as

$$\dot{\boldsymbol{q}}_{t_i} = R_{i-1}^n\dot{\boldsymbol{q}}_{t_{i-1}} + R_i^d\dot{\boldsymbol{q}}_{t_i} \tag{39}$$

where

$$R_i^n = \begin{bmatrix} I_{d_3} & P_i(\boldsymbol{h}_i) & \boldsymbol{T}_iKA_i & \boldsymbol{T}_iKL_i \\ 0 & 0 & 0 & 0 \\ 0 & 0 & 0 & 0 \\ 0 & 0 & 0 & 0 \end{bmatrix} \in \Re^{nq\times nq} \tag{40}$$

Thus, for the entire system,

$$\dot{\boldsymbol{q}}_t = R^n\dot{\boldsymbol{q}}_t + R^d\dot{\boldsymbol{q}}, \qquad \dot{\boldsymbol{q}}_t = \left(I_{d_{nqq}} - R^n\right)^{-1}R^d\dot{\boldsymbol{q}} \tag{41}$$

where

$$R^n = \begin{bmatrix} 0 & 0 & 0 & \cdots & 0 \\ R_1^n & 0 & 0 & \cdots & 0 \\ 0 & R_2^n & 0 & \cdots & 0 \\ \vdots & \vdots & \ddots & \ddots & \vdots \\ 0 & 0 & \cdots & R_{N-1}^n & 0 \end{bmatrix} \in \Re^{nqq\times nqq} \tag{42}$$

and

$$R^d = \begin{bmatrix} R_1^d & 0 & 0 & \cdots & 0 \\ 0 & R_2^d & 0 & \cdots & 0 \\ 0 & 0 & R_3^d & \cdots & 0 \\ \vdots & \vdots & \vdots & \ddots & \vdots \\ 0 & 0 & 0 & \cdots & R_N^d \end{bmatrix} \in \Re^{nqq\times nqq} \tag{43}$$

Equations of Motion

Returning to the expression for kinetic energy, after substituting Eq. (35) into Eq. (15) we get the first of two expressions for kinetic energy as

$$K_e = \tfrac{1}{2}\dot{\boldsymbol{q}}^T\left[R^{v^T}M_tR^v\right]\dot{\boldsymbol{q}} \tag{44}$$

Substituting Eq. (41) into Eq. (15), we have the second expression as

$$K_e = \tfrac{1}{2}\dot{\boldsymbol{q}}^T\left[\left(I_{d_{nqq}} - R^n\right)^{-1}R^d\right]^TM_t\left[\left(I_{d_{nqq}} - R^n\right)^{-1}R^d\right]\dot{\boldsymbol{q}} \tag{45}$$

Therefore we get two factorizations for the system's coupled mass matrix given as

$$M = R^{v^T}M_tR^v \tag{46}$$

$$= \left[\left(I_{d_{nqq}} - R^n\right)^{-1}R^d\right]^TM_t\left[\left(I_{d_{nqq}} - R^n\right)^{-1}R^d\right] \tag{47}$$

Inverting Eq. (47), we get

$$M^{-1} = (R^d)^{-1}\left(I_{d_{nqq}} - R^n\right)M_t^{-1}\left[(R^d)^{-1}\left(I_{d_{nqq}} - R^n\right)\right]^T \tag{48}$$

Since both R^d and M_t are block diagonal matrices, their inverse is simply the inverse of each block on the diagonal. Also, each block is $nq\times nq$ and is independent of the number of bodies in the whole system; thus the inversion of M is an $\mathcal{O}(N)$ operation.

The equations of motion are derived with a time-dependent offset of the tether attachment point $\boldsymbol{d}_i$, which is treated as a generalized coordinate. However, one may constrain it to a fixed or time-specified value. This is achieved through the introduction of Lagrangian multipliers. One begins by assigning the multipliers to all of the $\boldsymbol{d}$ equations. Thus, letting $\boldsymbol{f} = \boldsymbol{F} - \boldsymbol{Q}$ gives

$$M\ddot{\boldsymbol{q}} + \boldsymbol{f} = P^c\boldsymbol{\Lambda} \tag{49}$$

where $\Lambda \in \Re^{3N\times 1}$ is the vector of Lagrangian multipliers and P^c is the permutation matrix assigning the appropriate Λ_i to its corresponding $\boldsymbol{d}_i$ equation. Inverting M and premultiplying both sides by P^{cT} gives

$$\begin{aligned} P^{cT}(\ddot{\boldsymbol{q}} + M^{-1}\boldsymbol{f}) &= [P^{cT}M^{-1}P^c]\boldsymbol{\Lambda} \\ \left(\ddot{\boldsymbol{d}}_c + P^{cT}M^{-1}\boldsymbol{f}\right) &= [P^{cT}M^{-1}P^c]\boldsymbol{\Lambda} \end{aligned} \tag{50}$$

where $\ddot{\boldsymbol{d}}_c$ is the desired offset acceleration vector. Note that both $\ddot{\boldsymbol{d}}_c$ and $P^{cT}M^{-1}\boldsymbol{f}$ are known. Thus, the solution for $\boldsymbol{\Lambda}$ has the form

$$\boldsymbol{\Lambda} = [P^{cT}M^{-1}P^c]^{-1}\left(\ddot{\boldsymbol{d}}_c + P^{cT}M^{-1}\boldsymbol{f}\right) \tag{51}$$

Now, substituting Eq. (51) into Eq. (49) and rearranging the terms gives

$$\begin{aligned} \ddot{\boldsymbol{q}} &= \mathcal{S}(\boldsymbol{f}, M \mid \ddot{\boldsymbol{d}}_c) \\ &= -M^{-1}\boldsymbol{f} + M^{-1}P^c[P^{cT}M^{-1}P^c]^{-1}\left(\ddot{\boldsymbol{d}}_c + P^{cT}M^{-1}\boldsymbol{f}\right) \end{aligned} \tag{52}$$

which is the new constrained vector equation of motion with an offset specified by $\ddot{\boldsymbol{d}}_c$. It is interesting to note that, by explicitly substituting the constraint (dependent) equations into the independent ones, the need for constraint stabilization, introduced in Ref. (3), is circumvented.

Results and Discussion

The equations of motion were coded in Fortran and numerically integrated for a wide range of system parameters and initial conditions to illustrate their versatility. The modal integrals presented in Eqs. (19) and (20) are explicitly evaluated off line using a symbolic integration package, further improving overall computational performance. For brevity, only a few typical cases are reported to help establish trends.

Two system configurations are considered: the space station platform-based tethered satellite system (STSS) and the proposed BICEPS (bistatic Canadian experiment on plasmas in space) configuration. Both represent three-body systems, i.e., two end bodies

with an interconnecting tether. However, they exhibit significantly different responses because of the difference in their system configuration. The spin (cartwheeling) motion about the orbit normal during the BICEPS mission (Fig. 3) is unique to the tethered satellite systems.

Space Station-Based Tethered Satellite System

The numerical values used in the analysis of the STSS are as follows.

Platform inertia:

$$I_1 = \begin{bmatrix} 1{,}091{,}430 & -8135 & 328{,}108 \\ -8135 & 8{,}646{,}050 & 27{,}116 \\ 328{,}108 & 27{,}116 & 8{,}286{,}760 \end{bmatrix} \text{kg} \cdot \text{m}^2$$

Subsatellite inertia:

$$I_2 = \begin{bmatrix} 200 & 0 & 0 \\ 0 & 400 & 0 \\ 0 & 0 & 400 \end{bmatrix} \text{kg} \cdot \text{m}^2$$

Platform mass: $m_1 = 90{,}000$ kg
Subsatellite mass: $m_2 = 500$ kg
Tether flexural rigidity: $E_t A_t = 61{,}645$ N
Tether linear density: $\rho_t = 4.9$ kg/km
Tether structural damping coefficient: $\eta_d = 0.5\%$

The pitch and roll angles of each link, as well as the tether deflections, are defined in Fig. 4.

The system is taken to be in a circular orbit, 289 km in altitude, with an orbital period of 90.3 min. Only the first mode of longitudinal and transverse vibrations is considered in the discretization because it contains most of the elastic energy and thus dominates the response of the flexible degrees of freedom. The attachment point of the tether is represented by the offset position $\boldsymbol{d}_2 = \{d_x, d_y, d_z\}^T$ at the platform end and fixed at an arbitrary point at the subsatellite end.

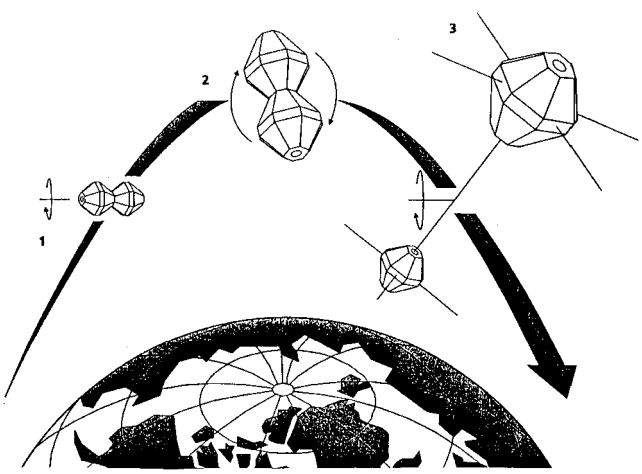

Fig. 3 Mission profile for the BICEPS satellite system: After separation, the subsatellite's spin direction is perpendicular to the orbit plane, point 1; internal dampers change to a flat spin, point 2; and a deployment maneuver utilizes angular momentum in the system, point 3.

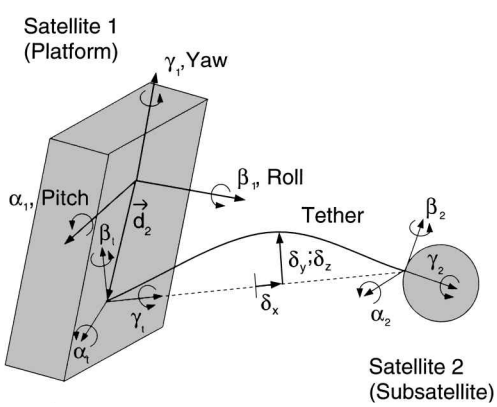

Fig. 4 Schematic diagram of the generalized coordinates used to describe the system dynamics.

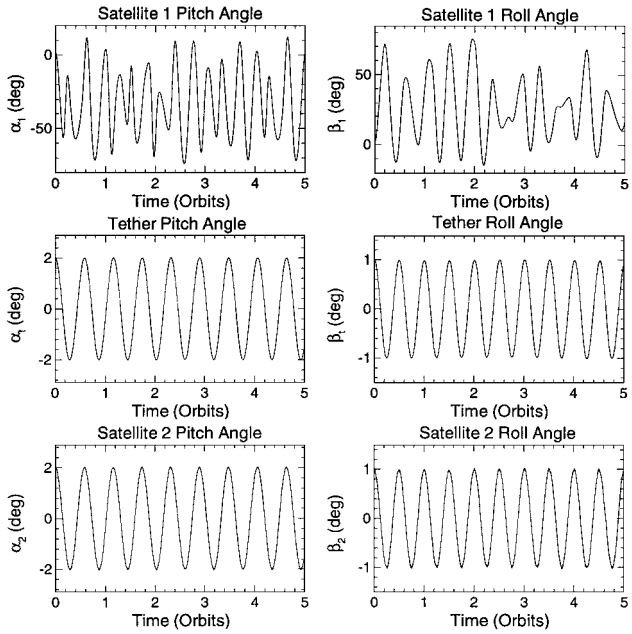

a) Attitude response

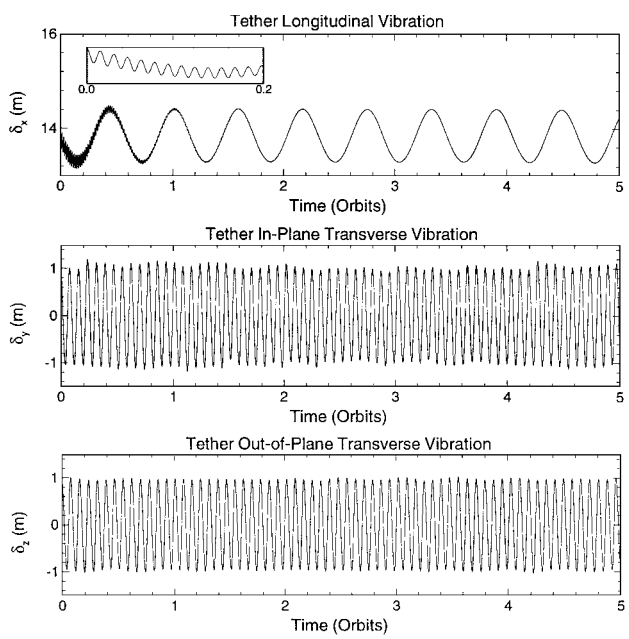

b) Vibration response

Fig. 5 Station-keeping dynamics of the three-body STSS with offset along the local horizontal, local vertical, and orbit normal directions. STSS configuration: three body; $\alpha_1(0) = \alpha_2(0) = \alpha_t(0) = 2$ deg, $\beta_1(0) = \beta_2(0) = \beta_t(0) = 1$ deg, $\delta_x(0) = 14$ m, $\delta_y(0) = \delta_z(0) = 1$ m, and $d_x(0) = d_y(0) = d_z(0) = 1$ m. Station keeping: $l_t = 20$ km.

Figure 5 presents the response of the STSS configuration with a fixed tether attachment point offset of 1 m in the local vertical x, local horizontal y, and orbit normal z directions. The tether length is held constant (station keeping) at 20 km. The platform, tether, and subsatellite are subjected to initial disturbances of 2 and 1 deg in the pitch and roll directions, respectively, as well as an initial longitudinal tether deflection of 14 m at the subsatellite end and an in-plane and out-of-plane deflection of 1 m at midlength. It is clear

that the pitch and roll motion of the space station is affected by the motion of the tether. This is due to the nonzero offset position of the tether attachment point, which provides a lever arm through which the tether tension produces a sufficiently strong moment to swing the station to over −70 deg in the pitch and +70 deg in the roll, resulting in a new platform equilibrium angle at ±30 deg. Similarly, the nonzero attachment point of the tether to the rigid end body causes satellite 2 to be completely dominated by the tether due to its smaller inertia. The longitudinal vibration, as expected, is composed of a high-frequency elastic component, which is attenuated due to internal damping, and a low-frequency contribution arising from coupling with the tether's in-plane libration. Note that only second-order damping is present in the transverse mode, resulting in very little attenuation. In fact, without any active or passive control scheme, the transverse mode may take an extremely long time (around two years) to completely vanish through structural damping. The tether libration motion is unaffected by the platform and subsatellite dynamics.

Next, the effect of tether deployment from 200 m to 20 km is considered. Initially there is no pitch or roll motion present, and there is an offset of 1 m along the local vertical. As shown in Fig. 6, the tether exhibits a large pitch displacement in the initial phases of deployment. This is due to the Coriolis force acting on the tether, which also affects the in-plane transverse vibration. Through coupling, the pitch motions of the rigid satellites follow the same trend as the tether. On the other hand, the roll motion of the tether is not affected by the Coriolis force, which only acts in the in-plane direction. There is a small excitation produced in the out-of-plane attitude and vibratory motion of the tether arising from the increase in roll for the platform at the terminal stages of deployment. From the time history of the longitudinal elastic deformation in the tether, it is apparent that the tether initially approaches the zero deflection mark δ_x corresponding to zero tension. Care must be exercised when choosing the deployment rate, especially at a shorter length, to maintain a positive tension at all times and, consequently, not to render the tether slack. However, as the tether elongates, its longitudinal static equilibrium also increases due to the increase in the gravity-gradient tether tension. In the case of retrieval (not shown here), the system becomes unstable if left uncontrolled. This suggests a need for a control strategy to regulate the system response to an acceptable value.

The deployment of both tethers in the double-pendulum configuration is presented in Fig. 7 for the case of the tether length varying from 200 m to 20 km. The pitch motion of the system is similar to that of the three-body case. The Coriolis effect forces the tether through a pitch motion of 50 deg, which in turn disturbs the rigid bodies' pitch motion due to the nonzero offset. On the other hand, the roll motion of both tethers is damped out to zero, from conservation of angular momentum, as the tether deploys, whereas that of the platform increases to about 20 deg. The end satellite is unaffected by the other links because the tether is attached to its center of mass, thus eliminating coupling. The flexible motion is similar to that of the three-body case.

BICEPS and OEDIPUS Configurations

To emphasize the relatively general character of the formulation and its potential to model a wide range of configurations, the case of deployment and cartwheeling of the BICEPS configuration is investigated. The numerical values used in the analysis are as follows.

Subsatellite inertias:

$$I_1 = I_2 = \begin{bmatrix} 5.9 & 0 & 0 \\ 0 & 36.6 & 0 \\ 0 & 0 & 39.2 \end{bmatrix} \text{kg} \cdot \text{m}^2$$

Subsatellite masses: $m_1 = m_2 = 200$ kg
Tether flexural rigidity: $E_t A_t = 61{,}645$ N
Tether linear density: $\rho_t = 3.0$ kg/km
Tether length: $l_t = 1$ km
Tether structural damping: $\eta_t = 0.5\%$

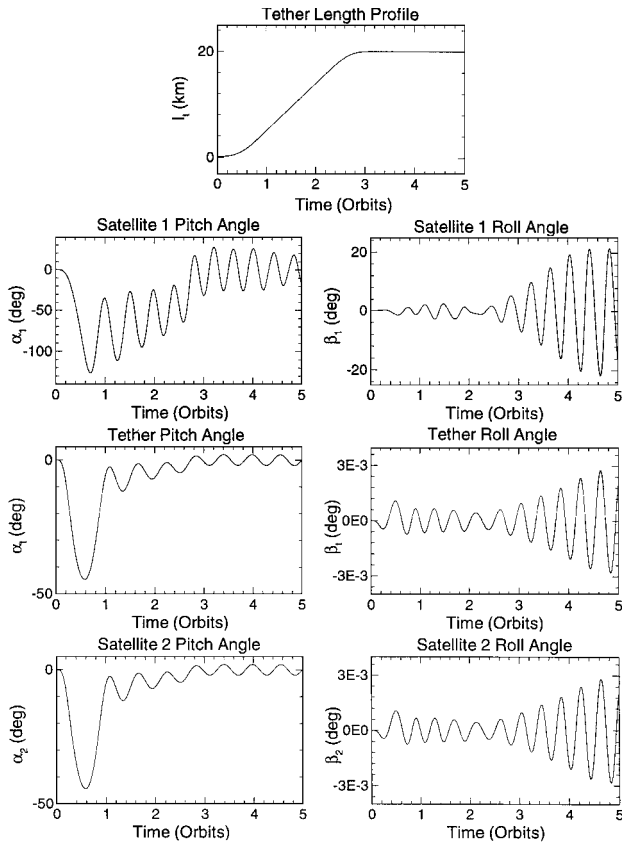

a) Attitude response

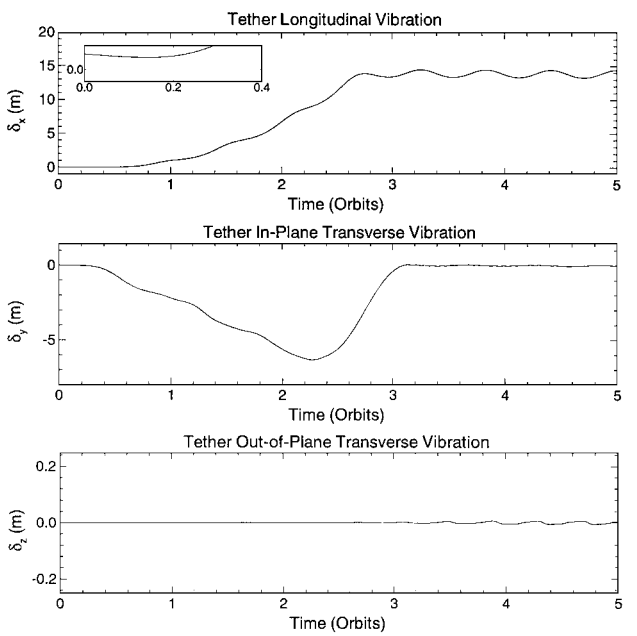

b) Vibration response

Fig. 6 Deployment dynamics of the three-body STSS with offset along the local vertical direction. STSS configuration: three body; $\alpha_1(0) = \alpha_2(0) = \alpha_t(0) = 0$, $\beta_1(0) = \beta_2(0) = \beta_t(0) = 0$, $\delta_x(0) = 1.304 \times 10^{-3}$ m, $\delta_y(0) = \delta_z(0) = 0$, and $d_x(0) = 1$ m, $d_y(0) = d_z(0) = 0$. Deployment: l_t = 0.2–20 km in 3.5 orbit.

Cartwheeling or spin about the orbit normal can be employed to assist deployment of the tether by utilizing the angular momentum and centrifugal acceleration of the system. The initial cartwheeling rate of the system is taken to be 5 deg/s. As can be expected, as the length of the tether increases, conservation of angular momentum dictates that $\dot{\alpha}$ must decrease proportionally to the square of the change in the tether length, as shown by the tether pitch time history in Fig. 8. Consequently, the system eventually stops

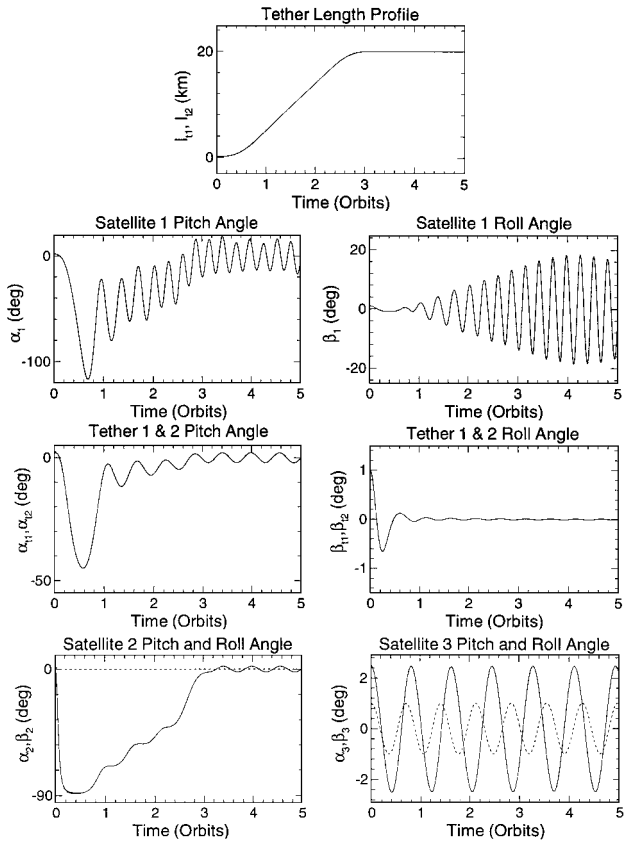

a) Attitude response: ——, pitch and - - - -, roll

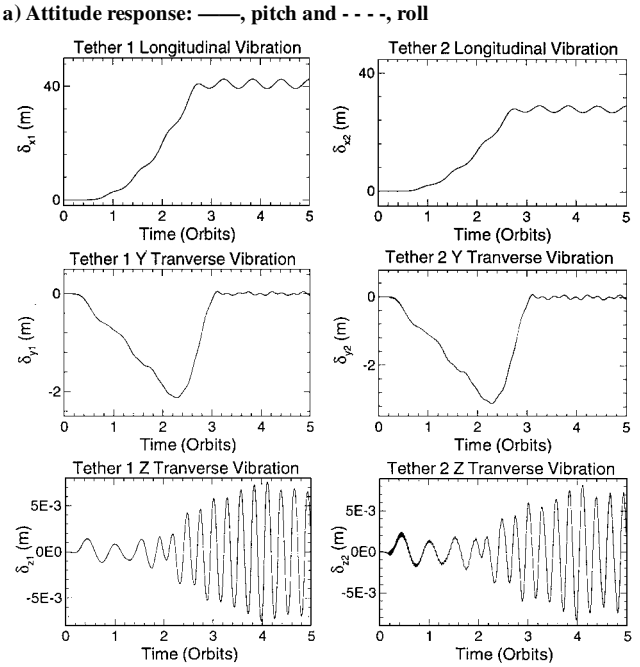

b) Vibration response

Fig. 7 Deployment dynamics of the five-body STSS with offset along the local vertical direction. STSS configuration: five body; $\alpha_1(0) = \alpha_2(0) = \alpha_{t1}(0) = 2$ deg, $\alpha_3(0) = \alpha_{t2}(0) = 2.5$ deg, $\beta_1(0) = \beta_2(0) = \beta_3(0) = \beta_{t1}(0) = \beta_{t2}(0) = 1$ deg, $\delta_2(0) = \delta_4(0) = \{1.304 \times 10^{-3}, 0, 0\}$ m, and $d_2(0) = d_4(0) = \{1, 0, 0\}$ m. Deployment: $l_{t1} = l_{t2} = 0.2$–20 km in 3.5 orbits.

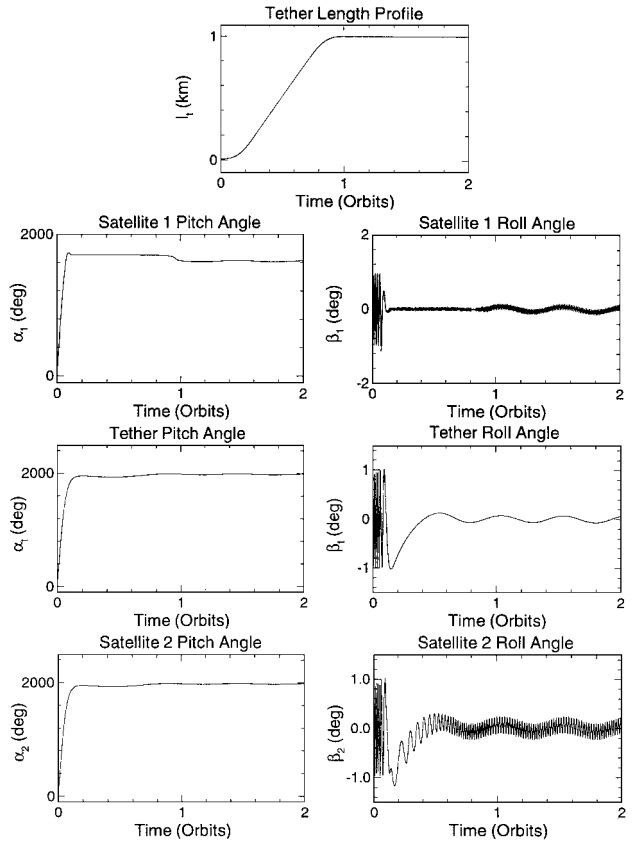

a) Attitude response

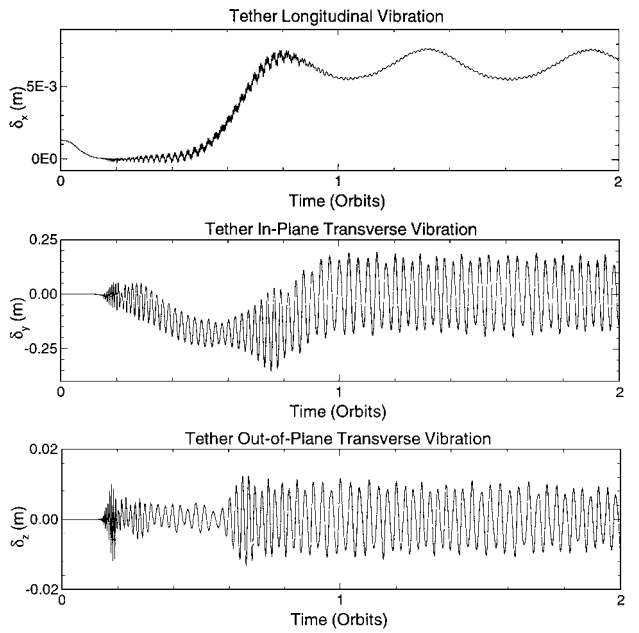

b) Vibration response

Fig. 8 Cartwheeling dynamics with deployment for the three-body BICEPS configuration with offset along the local vertical direction. BICEPS configuration: three body; $\alpha_1(0) = \alpha_2(0) = \alpha_t(0) = 2$ deg, $\dot{\alpha}_1(0) = \dot{\alpha}_2(0) = \dot{\alpha}_t(0) = 5$ deg/s, $\beta_1(0) = \beta_2(0) = \beta_t(0) = 1$ deg, $\delta_x(0) = 1.15 \times 10^{-3}$ m, $\delta_y(0) = \delta_z(0) = 0$, and $d_x(0) = 0.78$ m, $d_y(0) = d_z(0) = 0$. Cartwheeling deployment: $l_t = 10$ m to 1 km in 1 orbit.

rotating and simply oscillates about its new equilibrium position. However, caution must be exercised when cartwheeling the system to maintain the tether tension low, thus preventing elastic recoil once the rotation has stopped, which would otherwise render the tether slack.

A mission profile similar to BICEPS is the mission entitled Observation of Electrified Distributions of Ionospheric Plasmas—A Unique Strategy or OEDIPUS. What makes this mission unique is that it spins about its nominal tether length. The response of the system undergoing a spin rate of $\dot{\gamma} = 10$ deg/s is presented in Fig. 9 using the same parameters as those for the BICEPS configuration. Again, there is strong coupling between all three links due to the nonzero offset position. The spin motion has the effect of introducing additional frequency components in the tether's vibratory motion, which disturbs the librational motion of the subsatellites.

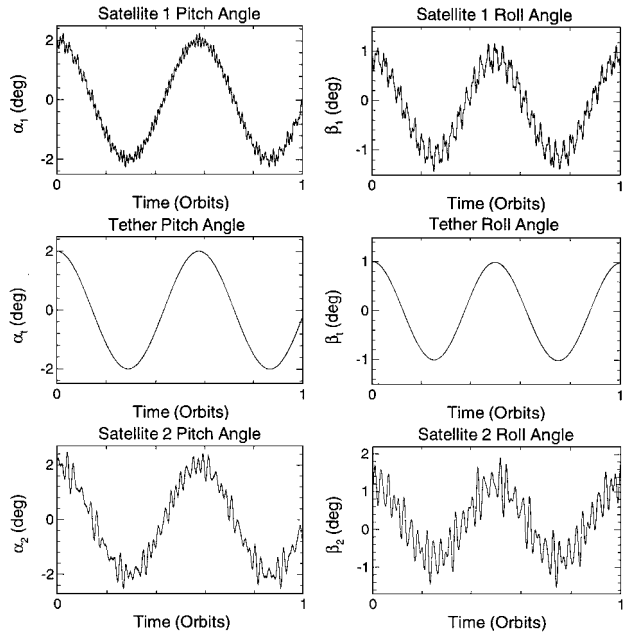

a) Attitude response

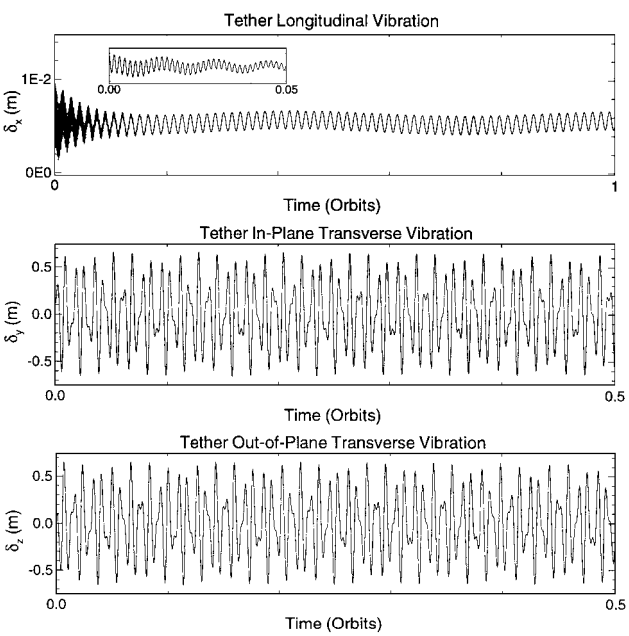

b) Vertical direction

Fig. 9 Spin dynamics ($\dot{\gamma}$ = 10 deg/s) of the three-body OEDIPUS configuration with offset along the local vertical direction. OEDIPUS configuration: three body; $\alpha_1(0) = \alpha_2(0) = \alpha_t(0) = 2$ deg, $\dot{\gamma}_1(0) = \dot{\gamma}_2(0) = \dot{\gamma}_t(0) = 10$ deg/s, $\beta_1(0) = \beta_2(0) = \beta_t(0) = 1$ deg, $\delta_x(0) = 1.2 \times 10^{-3}$ m, $\delta_y(0) = \delta_z(0) = 0.1$ m, and $d_x(0) = 0.78$ m, $d_y(0) = d_z(0) = 0$. Station keeping: $l_t = 1$ km.

Concluding Remarks

An order-N Lagrangian algorithm for the equations of motion of a flexible multibody tethered system is developed. The model considered is a multisatellite flexible tethered system forming a chain geometry, capable of deployment and retrieval. The tether attachment point to the end satellite is kept arbitrary and time varying. Furthermore, the model is capable of spin about an arbitrary axis, as in the case of the BICEPS mission, which cartwheels about the orbit normal, or its predecessor OEDIPUS-A/C, which spins about the nominal tether length. The tether flexibility is discretized using the assumed mode method.

The equations of motion are coded in Fortran with the modal integrals evaluated symbolically to improve the simulation performance. Two system configurations are considered: the space station-based tethered system and the BICEPS/OEDIPUS configuration. Both exhibit significantly different responses due to differences in their system properties and mission profiles. The general character of the formulation makes it applicable to a large class of systems of contemporary interest and can readily accommodate a wide variety of configurations as well as operational profiles.

Results of the parametric study clearly show the effect of the tether attachment point offset as well as coupling between the various degrees of freedom. They also bring to light the need for active control due to potentially undesirable attitude motion under critical combinations of system parameters and initial conditions. Similarly, the need for vibration control for the tether is also demonstrated. A vibration controller based on the tether's offset position and a nonlinear feedback controller for the system's attitude motion have been developed and will be the topic of discussion in the future.

References

[1]Keshmiri, M., and Misra, A. K., "A General Formulation for N-Body Tethered Satellite System Dynamics," *Advances in the Astronautical Sciences*, edited by A. K. Misra, V. J. Modi, R. Holdaway, and P. M. Bainum, Vol. 85, Pt. 1, American Astronautical Society, San Diego, CA, 1993, pp. 623–644.

[2]Misra, A. K., and Modi, V. J., "Three-Dimensional Dynamics and Control of Tether-Connected N-Body Systems," *Acta Astronautica*, Vol. 26, No. 2, 1992, pp. 77–84.

[3]Banerjee, A. K., and Do, V. N., "Deployment Control of a Cable Connecting a Ship to an Underwater Vehicle," *Journal of Guidance, Control, and Dynamics*, Vol. 17, No. 6, 1994, pp. 1327–1332.

[4]Fu, K. S., Gonzalez, R. C., and Lee, C. S. G., *Robotics: Control, Sensing, Vision, and Intelligence*, McGraw–Hill, New York, 1987, pp. 103–124.

[5]Hollerbach, J. M., "A Recursive Lagrangian Formulation of Manipulator Dynamics and a Comparative Study of Dynamics Formulation Complexity," *IEEE Transactions on Systems, Man, and Cybernetics*, Vol. SMC-10, No. 11, 1980, pp. 730–736.

[6]Rosenthal, D. E., "An Order *n* Formulation for Robotic Systems," *Journal of the Astronautical Sciences*, Vol. 38, No. 4, 1990, pp. 511–529.

[7]Banerjee, A. K., "Block-Diagonal Equations for Multibody Elastodynamics with Geometric Stiffness and Constraints," *Journal of Guidance, Control, and Dynamics*, Vol. 16, No. 6, 1993, pp. 1092–1100.

[8]Keat, J. E., "Multibody System Order *n* Dynamics Formulation Based on Velocity Transform Method," *Journal of Guidance, Control, and Dynamics*, Vol. 13, No. 2, 1990, pp. 207–212.

[9]Rodriguez, G., and Kreutz-Delgato, K., "Spatial Operator Factorization and Inversion of the Manipulator Mass Matrix," *IEEE Transactions on Robotics and Automation*, Vol. 8, No. 1, 1992, pp. 65–76.

[10]Jain, A., and Rodriguez, G., "Recursive Dynamics Algorithm for Multibody Systems with Prescribed Motion," *Journal of Guidance, Control, and Dynamics*, Vol. 16, No. 5, 1993, pp. 830–837.

[11]Kurdila, A. J., Menon, R. G., and Sunkel, J. W., "Nonrecursive Order *N* Formulation of Multibody Dynamics," *Journal of Guidance, Control, and Dynamics*, Vol. 16, No. 5, 1993, pp. 838–844.

[12]Pradhan, S., Modi, V. J., and Misra, A. K., "An Order *N* Dynamics Formulation of Flexible Multibody Systems in Tree Topology—The Lagrangian Approach," *Proceedings of the AIAA/AAS Astrodynamics Specialist Conference*, AIAA, Reston, VA, 1996, pp. 480–490 (AIAA Paper 96-3624); also "Order *N* Formulation for Flexible Multibody Systems in Tree Topology: Lagrangian Approach," *Journal of Guidance, Control, and Dynamics*, Vol. 20, No. 4, 1997, pp. 665–672.

[13]Pradhan, S., Modi, V. J., and Misra, A. K., "On the Inverse Control of the Tethered Satellite Systems," *Journal of the Astronautical Sciences*, Vol. 43, No. 2, 1995, pp. 179–193.

[14]Kim, E., and Vadali, S. R., "Modeling Issues Related to Retrieval of Flexible Tethered Satellite Systems," *Journal of Guidance, Control, and Dynamics*, Vol. 18, No. 5, 1995, pp. 1169–1176.

[15]Wu, S., Chang, C., and Housner, J. M., "Finite Element Approach for Transient Analysis of Multibody Systems," *Journal of Guidance, Control, and Dynamics*, Vol. 15, No. 4, 1992, pp. 847–854.

[16]Xu, D. M., "The Dynamics and Control of the Shuttle Supported Tethered Subsatellite System," Ph.D. Thesis, Dept. of Mechanical Engineering, McGill Univ., Montreal, PQ, Canada, Nov. 1984.

[17]Hughes, P. C., *Spacecraft Attitude Dynamics*, Wiley, New York, 1992, pp. 7–38.